

# The $J_{i,j} = \pm J$ Ising learning machine

O Duranthon<sup>1</sup> and M Marsili<sup>2,3</sup>

<sup>1</sup>École Normale Supérieure, Paris, France

<sup>2</sup>The Abdus Salam International Center for Theoretical Physics, Trieste, Italy

<sup>3</sup>Istituto Nazionale di Fisica Nucleare (INFN), Sezione di Trieste, Italy

July 19, 2022

## Abstract

Optimal Learning Machines (OLM) are systems that extract maximally informative representation from data. At a given resolution, they maximise the relevance, which is the entropy of their energy distribution. We show that the relevance lower bounds the mutual information between the representation and the hidden features that it extracts from data. In order to understand their peculiar properties, we study  $J_{i,j} = \pm J$  fully connected Ising models and contrast their properties with the Ising ferromagnet ( $J_{i,j} = J$ ). The main finding is that optimal Ising learning machines are characterised by inhomogeneous distributions of couplings and that their relevance increases as  $h_E \log n$  with the number  $n$  of spins, with  $h_E > 1$ . This contrasts with the behaviour of ferromagnets or spin glasses, that we argue have  $h_E \leq 1$ . Learning performance is related to sub-extensive features of the models that are elusive to a thermodynamic treatment. Indeed, we find models with  $h_E \geq 1$  that differ from the Ising ferromagnet by a sub-extensive number of couplings and that share the same thermodynamic properties with it. We also exhibit an architecture which suggests that superior learning performance does not require fine tuning to a critical point. The space of couplings of OLM is dominated by a large connected component.

Statistical mechanics models have been used in statistical learning since the pioneering works on associative memory [1] and on Boltzmann Learning Machines [2]. Many attempts to make sense of the spectacular performance of learning machines, such as deep neural networks, have focused on understanding their statistical mechanics properties (see e.g. [3, 4, 5, 6, 7]), as compared e.g. to spin glasses [8]. It is widely believed that learning machines are characterised by some typical properties, such as the compositional phase discussed in [3], wide flat free energy minima [4] or criticality [6]. Yet, these properties only emerge after the interaction parameters have been learned from highly structured datasets [5]. In addition, the properties of learning machines also depend on what measure of error or likelihood is used in supervised or unsupervised learning, respectively. This makes it hard to discuss the typical properties of learned models without reference to the particular dataset on which the model is trained, or on the objective function assumed.

Here we take the view, recently suggested in [9], that learning machines approximate an ideal limit of what we shall call Optimal Learning Machines (OLM). In this view, the energy

$E_s = -\log p(s)$  is the coding cost associated to a microscopic state  $s$ . Hence the average energy

$$\langle E \rangle = - \sum_s p(s) \log p(s) \equiv H[s] \quad (1)$$

is a measure of the resolution of the representation encoded in the model. The entropy of the energy distribution

$$H[E] = - \sum_E p(E) \log p(E) \quad (2)$$

instead provides a quantitative measure of the information that the model contains on the generating process of the data, and is henceforth called *relevance*. OLM are statistical mechanics models that maximise the relevance at a given resolution  $H[s]$ . In other words, the architecture of these models are such that the distribution of their energy levels is as broad as possible. This allows one to describe the properties of OLM without reference to the data with which they have been trained. This apparently paradoxical fact is rooted on the assumption that the data with which the learning machine is trained contains a rich structure and that the goal of learning is precisely to decompose this structure into a set of hidden features. This argument, which is developed in the next section, shows that the relevance  $H[E]$  is a lower bound to the amount of information that the representation contains on the hidden features. Hence *models with maximal relevance, at a fixed resolution, are those that are mostly informative on the features hidden in the data*. As a corollary, OLM are machines that extract the most compressed representations from data, with an information content on the features which is at least of  $H[E]$  bits.

This requirement implies an exponential distribution of energy levels, which is equivalent to statistical criticality [9]. The fact that this is a widely observed statistical regularity in efficient representations [6, 10, 11], corroborates the use of the principle of maximal relevance as a tool to understand learning machines.

Maximal relevance is a very general principle. The aim of this paper is to investigate it in the context of a specific class of models, the  $J_{i,j} = \pm J$  fully connected Ising models, in order to understand what architectures OLM correspond to. In particular, we discuss the statistical mechanics properties of OLM within this class, in order to contrast the properties of Ising OLM with those of well known models, such as the mean field Ising ferromagnet and the  $J_{i,j} = \pm J$  spin glass. Our main findings are that *i)* properties that make models good learning machines are related to sub-leading terms in a statistical mechanics analysis and are not accessible to standard approaches, *ii)* OLM feature heterogeneous architectures and *iii)* their properties are not necessarily related to models being poised at a critical point.

The next section discusses the principle of maximal relevance in a general context of feature extraction in learning. The following one, introduces the Ising learning machine. It first discusses OLM in this class for small systems through exact enumeration and then few specific architectures for large systems. We summarise and comment our results in the concluding section.

## 1 Relevance maximisation and hidden features

Let us assume that data points  $\vec{x} = (x_1, \dots, x_d)$  are generated as draws from an unknown distribution  $p(\vec{x})$  that is characterised by a rich structure of dependence between the components  $x_a$ . For example, the benchmark MNIST dataset of hand written digits has  $d = 28 \times 28 = 784$  pixels, for each of which, the grey scale is codified in an integer  $\vec{x}_a$  in the

range  $[0, 255]$ . Nearby pixels have typically similar values of  $x_a$ , hence  $p(\vec{x})$  should be a model of strongly interacting variables.

We focus on stochastic models, such as Restricted Boltzmann Machines (RBM) or Deep Belief Networks (DBN), with a discrete number of internal states. The goal of learning is to find a statistical model  $p(s)$  over a discrete variables  $s$ , and a mapping  $p(\vec{x}|s)$  from  $s$  to  $\vec{x}$ , such that the generating distribution

$$p_{\text{gen}}(\vec{x}) = \sum_s p(\vec{x}|s)p(s)$$

is as close as possible to the empirical one (in unsupervised learning), or that the representation approximates a functional relation  $\underline{x}_{\text{out}} = f(\underline{x}_{\text{in}})$  between two parts of the data  $\vec{x} = (\underline{x}_{\text{in}}, \underline{x}_{\text{out}})$  as well as possible (in supervised learning). The objective function employed may differ, yet in both cases the aim is that of approximating the unknown generative process  $p(\vec{x}) \approx p_{\text{gen}}(\vec{x})$  as closely as possible (or at least that part which is responsible for the dependence of the output  $\underline{x}_{\text{out}}$  on the input  $\underline{x}_{\text{in}}$ ). Here we describe the outcome of this process in abstract terms, in order to derive a lower bound on the information learned.

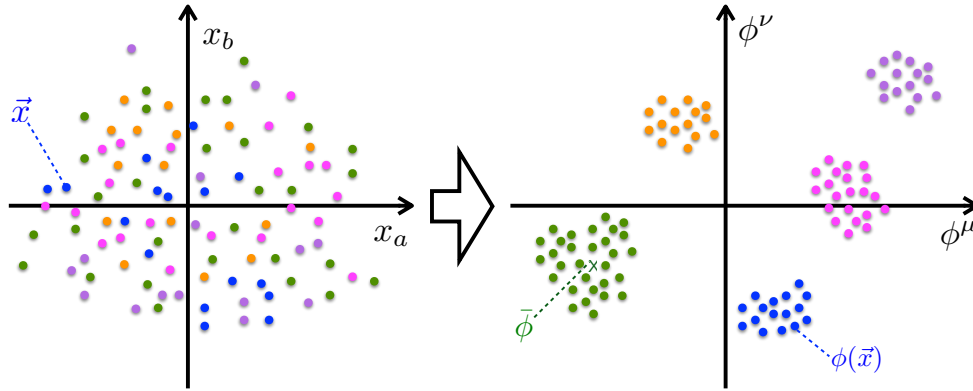


FIGURE 1. Sketch of the map of a dataset to the space of features. Points with similar features  $\phi(s(\vec{x})) \approx \bar{\phi}$  are statistically identical. Statistically distinct points are distinguished by a significant variation  $\delta\phi$  of the feature vector.

Let us assume that the structure of dependencies in  $p(\vec{x})$  can be represented in terms of a vector of hidden features  $\phi = (\phi^1, \dots, \phi^m)$ , as shown in Fig. 1, so that *i*) points with a similar value  $\phi(\vec{x}) \approx \bar{\phi}$  correspond to statistically undistinguishable points in the data, and *ii*) the variation  $\delta\bar{\phi}$  captures the variability across qualitatively different points  $\vec{x}$ .

Let us now relate this picture to the properties of a representation  $p(s)$  at a given resolution<sup>1</sup>  $H[s]$ . Features can be defined in terms of a vector of functions  $\phi(s)$  defined on the states  $s$  of the machine, as

$$\phi(\vec{x}) = \sum_s \phi(s)p(s|\vec{x}). \quad (3)$$

Note that  $p(s|\vec{x})$  depends on the unknown distribution  $p(\vec{x})$  and so does  $\phi(\vec{x})$ , instead  $\phi(s)$  is defined in terms of the representation  $s$ , so it is in principle accessible.

<sup>1</sup> $H[s]$  is determined by the specific architecture, e.g. by the number of hidden nodes in RBMs.

In the representation space  $s$ , the picture in Fig. 1 translates in the decomposition

$$p(s) = \int d\bar{\phi} p(s|\bar{\phi})p(\bar{\phi}) \quad (4)$$

where  $p(s|\bar{\phi})$  is such that<sup>2</sup>

$$\sum_s \phi(s)p(s|\bar{\phi}) = \bar{\phi}. \quad (5)$$

The requirement *i*) implies that the conditional distribution  $p(s|\bar{\phi})$  should contain no useful information or, conversely, that the expected values  $\bar{\phi}$  contains all useful information to determine  $p(s|\bar{\phi})$ . The maximum entropy principle implies that<sup>3</sup>

$$p(s|\bar{\phi}) = \frac{1}{Z(g(\bar{\phi}))} e^{\sum_{\mu=1}^m g^{\mu}(\bar{\phi})\phi^{\mu}(s)}, \quad (6)$$

where  $g^{\mu}(\bar{\phi})$  is fixed by the constraint in Eq. (5). In information theoretic terms,  $\phi(s)$  are the minimal sufficient statistics of  $p(s|\bar{\phi})$ .

A consequence of Eq. (6) is that, all points  $s$  with the same features  $\phi(s)$  have the same probability, or equivalently, the energy

$$E_s = -\log \int d\bar{\phi} \frac{p(\bar{\phi})}{Z(g(\bar{\phi}))} e^{\sum_{\mu} g^{\mu}(\bar{\phi})\phi^{\mu}(s)} = \mathcal{E}(\phi(s)) \quad (7)$$

is a function of  $\phi(s)$ . In other words, the statistical dependence of the variables can be represented as the Markov chain<sup>4</sup>

$$\vec{x} \rightarrow s \rightarrow \phi \rightarrow E. \quad (8)$$

The data processing inequality [13] then implies that

$$I(s, \phi) \geq I(s, E) = H[E], \quad (9)$$

where the last equality comes from the fact that  $I(s, E) = H[E] - H[E|s]$  and  $H[E|s] = 0$ . Therefore,  $H[E]$  provides a lower bound to the information that the representation extracts on the hidden features. Machines with a maximal relevance  $H[E]$ , at a fixed resolution  $H[s]$ , push this lower bound as much as possible thereby achieving maximally informative representations.

The relation (8) also implies that  $I(s, \phi) \geq I(\vec{x}, \phi)$ , where the equality holds when the internal state  $s$  of the learning machine is a deterministic function  $s(\vec{x})$  of the data. This suggests that the probabilistic nature of the mapping  $\vec{x} \rightarrow s$  is related to overfitting, i.e. to cases where the machine extracts more information on features than the amount  $I(\vec{x}, \phi)$  contained in the data. Interestingly, in probabilistic learning machines such as RBMs or DBNs, the *clamped* distribution  $p(s|\vec{x})$  in hidden layers with good generating capacity is highly peaked on a single state  $s(\vec{x})$ , i.e. it is close to being deterministic. Notice also that

$$I(\vec{x}, \phi) \geq I(\vec{x}, E) = H[E] - H[E|\vec{x}]. \quad (10)$$

<sup>2</sup>Note that  $\bar{\phi}$  is the same in both representations. Indeed, given the distribution  $p(\vec{x}|\bar{\phi})$  of all points with  $\phi(\vec{x}) \approx \bar{\phi}$ , as long as  $\int d\vec{x} \phi(\vec{x})p(\vec{x}|\bar{\phi}) = \bar{\phi}$ , one recovers Eq. (5) using Eq. (3) and  $p(s|\bar{\phi}) = \int d\vec{x} p(s|\vec{x})p(\vec{x}|\bar{\phi})$ .

<sup>3</sup>It's interesting to remark, in passing, the similarity of Eq. (6) with models discussed in Ref. [12]. Ref. [12] shows that hidden variables in statistical models generate Zipf's law. The occurrence of Zipf's law in RBMs [6] is a natural manifestation of this observation, in the present framework.

<sup>4</sup>The notation  $z \rightarrow y \rightarrow w$  implies that condition on  $y$ ,  $z$  and  $y$  are independent, or that  $I(z, w|y) = 0$  [13]. This holds trivially true if  $w$  is a function of  $y$ , because then  $w|y$  is not a random variable.

So when the internal state  $s$  of the learning machine is a deterministic function  $s(\vec{x})$  of the data, then  $H[E|\vec{x}] = 0$ , and the relevance provides also a lower bound on the information that the data contain on the features.

Notice that  $H[s|\phi]$  provides a measure of that part of  $H[s]$  which is not informative on the features. By Eq. (9), this is upper bounded by  $H[s|E]$ . Maximising  $H[E]$  at fixed resolution  $H[s]$  implies minimising  $H[s|E] \geq H[s|\phi]$ , i.e. squeezing noise out of the representation.

In this picture, an alternative definition of OLM, are machines that extract the most compressed representations from data, at a minimal information content  $H[E]$  on the features

$$\min_{I(s,\phi) \geq H[E]} H[s]. \quad (11)$$

## 2 The optimal Ising learning machine

We consider a model of  $n$  spins  $s = (s_1, \dots, s_n)$ ,  $s_i = \pm 1$ , defined by an Hamiltonian

$$\mathcal{H}(s) = - \sum_{i < j} J_{i,j} s_i s_j, \quad (12)$$

where the couplings take values  $J_{i,j} \in \{\pm J\}$ . This induces a Gibbs measure

$$p(s) = \frac{1}{Z} e^{-\mathcal{H}(s)} \quad (13)$$

on the space of configurations. As discussed above, we define the energy as the coding cost  $E_s = -\log p(s) = \mathcal{H}(s) + \log Z$ , and address the optimisation problem

$$\mathcal{J} = \arg \max_{\hat{J}: H[s] = \bar{E}} H[E], \quad (14)$$

where the maximum is taken over all matrices with elements  $J_{i,j} = \pm J$ , and on  $J$ .  $\mathcal{J}$  is the subset of such matrices that achieve a maximal value of  $H[E]$ . We remark that this is a dual problem with respect to that addressed in statistical physics<sup>5</sup>.

In order to compute  $H[E]$  as a function of  $\hat{J}$ , we find the distribution of the energy as

$$p(E) = \sum_s p(s) \delta(E - E_s) = W(E) e^{-E} \quad (16)$$

where  $W(E)$  is the number of states  $s$  with energy  $E_s = E$ . From this and Eq. (2), we compute the value of  $H[E]$ .

The rest of this paper is devoted to describe the trade-off between  $H[E]$  and  $H[s]$  for models in the class of Eq. (12). Since  $H[s] \leq n \log 2$  within this class, we shall discuss the rescaled resolution

$$h_s = \frac{H[s]}{n \log 2}. \quad (17)$$

---

<sup>5</sup>The physical properties of a system with Hamiltonian  $E_s$  are derived, from the maximum entropy principle, i.e. finding the distribution  $p(s)$  over microscopic states  $s$  that maximises the entropy  $H[s]$  at a given value of the average energy  $\langle E \rangle = \sum_s p(s) E_s = \bar{E}$ . As a result, the distribution over the set of  $2^n$  configurations is

$$P(s) = \frac{1}{Z} e^{-\beta E_s}, \quad Z = \sum_s e^{-E_s} \quad (15)$$

with  $Z$  being the partition function and  $\beta$  is adjusted to satisfy the constraint  $\langle E \rangle = \bar{E}$ . Typical states drawn from  $p(s)$  have all the same energy  $E_s \approx \bar{E}$ . Here the maximisation is carried out over the Hamiltonian at fixed entropy  $H[s]$ , with  $p(s) = e^{-E_s}$ .

Analogously, we observe that  $E_s/J$  takes value only on the integers and  $|E_s|/J \leq n(n-1)/2$ , which justifies the introduction of the rescaled relevance

$$h_E = \frac{H[E]}{\log n} \quad (18)$$

that takes values in the interval  $[0, 2)$ . The sub-extensive nature of  $H[E]$  suggests that properties that contribute to the relevance of a model may not be accessible to saddle point analysis of the partition function, that focuses only the leading extensive terms.

Both  $h_s$  and  $h_E$  only depend on  $\hat{J}$  through the degeneracy  $W(E)$  of energy levels.  $W(E)$  is invariant under the permutation of the spins. Hence if  $\hat{J} \in \mathcal{J}$  then also the matrix with elements  $J_{\pi(i), \pi(j)}$  is a solution, where  $\pi(i)$  is a permutation of the indices  $i = 1, \dots, n$ . Also, matrices  $\hat{J}$  and  $\hat{J}'$  that are related by a gauge symmetry  $J'_{i,j} = \tau_i J_{i,j} \tau_j$ , with  $\tau_i = \pm 1$ , have the same  $W(E)$ . Hence, if  $\hat{J} \in \mathcal{J}$ , then also its gauge transformed  $\hat{J}'$  belongs to  $\mathcal{J}$ . We partially exploit these symmetries by fixing the gauge with the choice  $J_{1,j} = 1$  for all  $j \neq 1$ . Henceforth we shall focus on the reduced set  $\mathcal{J}$  of matrices with this choice of the gauge.

An interesting point that we shall discuss is how the set  $\mathcal{J}$  of solutions  $\hat{J}$  are organised, i.e. whether they correspond to isolated maxima or whether they form a compact set of nearby solutions in terms of local moves that involves the change of few  $J_{i,j}$ 's. This may shed light on the accessibility of solutions of Eq. (14) to learning rules such as stochastic gradient descent.

### 3 Exact enumeration for small systems

Each model in Eq. (12) is defined by a choice of the sign of the  $n(n-1)/2$  couplings  $J_{i,j}$  and by the strength  $J$  of the couplings. There are  $2^{n(n-1)/2}$  possible ways of choosing the signs. Yet, this number can be reduced by fixing the gauge. We were able to compute  $h_E$  as a function of  $h_s$  for all models up to  $n = 9$  spins. This allows us to find those models that achieve a maximal  $h_E$  for a given resolution  $h_s$ .

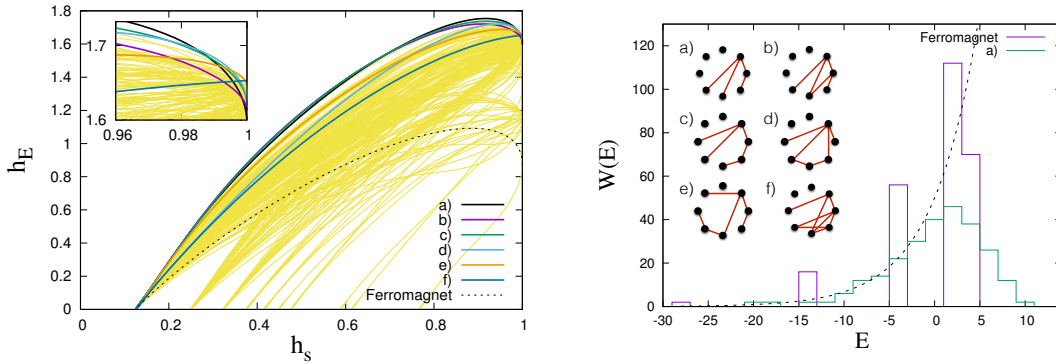


FIGURE 2. (Left)  $h_E$  vs  $h_s$  for all models with  $n = 8$  spins. The curves highlighted correspond to the models shown on the right plot (only  $J_{i,j} < 0$  are shown as red links). The dotted line corresponds to the ferromagnet. The inset magnifies the region around  $h_s = 1$ . (Right) Degeneracy  $W(E)$  of energy levels for the model  $a)$  (top left) and for the ferromagnet. The dotted line corresponds to an exponential  $W(E) = W_0 e^{\nu E}$  with  $\nu = 0.2$ .

Representative results are shown in Fig. 2 for  $n = 8$ . There are  $M = 219$  different curves in the left panel, each corresponding to a different degeneracy  $W(E)$  of energy levels. The

$n$	$M$
3	2
4	3
5	7
6	16
7	54
8	219
9	1625

TABLE 1. The number of different  $W(E)$  for  $n$  ranging from 3 to 9.

value of  $M$  for different values of  $n$  is shown in Table 1. Fig. 2(left) shows, in particular, the six functions  $h_E$  that achieve maximal relevance for some value of  $h_s$ . A representative choice of the corresponding matrix  $\hat{J} \in \mathcal{J}$  is shown in the right part of Fig. 2. Fig. 2(right) shows the degeneracy  $W(E)$  for model *a*) (top left in Fig. 2 right). As a comparison, Fig. 2 also shows the curve  $h_E(h_s)$  (left) and the degeneracy  $W(E)$  for the ferromagnet ( $J_{i,j} = J \forall i, j$ ).

The architectures that achieve maximal relevance, that we identify with OLM, have the following distinctive properties: *i*) the large majority of the couplings  $J_{i,j}$  are positive, which means that OLM are close to ferromagnetic models. Indeed, the ground state of all OLM are the same as that of the ferromagnet. Yet, *ii*) the relevance for OLM achieves a much higher value than for the ferromagnetic model (dotted line in Fig. 2 left). This is consistent with the fact that the degeneracy for the ferromagnet is concentrated on few values of  $E$ , whereas for OLM it spreads over a larger number of values of  $E$ . The degeneracy  $W(E)$  is consistent with an exponential behaviour, as predicted in Ref. [9]. Finally *iii*) the architectures of OLM appear to be rather inhomogeneous, with negative  $J_{i,j}$  impinging on a small subset of nodes. Such a low degree of symmetry, is probably related to the fact that the number  $|\mathcal{J}|$  of matrices  $\hat{J}$  that share the same  $W(E)$  of OLM is rather large (see Table 2).

It is interesting to analyse how the set  $\mathcal{J}$  is structured with respect to a single rewiring of a negative  $J_{i,j}$ , because this may shed light on the accessibility of OLM under a local learning dynamics during training. We find (see Table 2 for  $n = 8$ ) that the multiplicity of these sets decreases with the value of  $h_s$  for which these OLM are optimal. These sets are dominated by a single largest component which is suggestive of the wide flat minima discussed in Ref. [4]. This observation is corroborated by the fact that any OLM  $\in [a, b, \dots, f]$  can be obtained by a different OLM by local moves, such as the addition and/or the rewiring of a single negative  $J_{i,j}$ . As  $h_s$  decreases, we see a tendency of the set to shrink and to fragment in different connected components.

## 4 Some particular architectures

This section analyses specific architectures for which the curve  $h_E(h_s)$  can be computed for large values of  $n$ . We start with the ferromagnet, that although far from an optimal architecture, will serve as a benchmark.



OLM	$ \mathcal{J} $	connected components	$h_s$
f	80640	$80640 \times 1$	$[0.999, 1]$
e	40320	$35280 \times 1 + 5040 \times 1$	$[0.995, 0.999]$
d	10080	$10080 \times 1$	$[0.984, 0.995]$
a	3360	$2940 \times 1 + 12 \times 35$	$[0.71, 0.984]$
c	10080	$7560 \times 1 + 1260 \times 1 + 12 \times 105$	$[0.62, 0.71]$
b	3360	$2100 \times 1 + 420 \times 2 + 4 \times 105$	$[0.22, 0.62]$

TABLE 2. Structure of the set of  $\hat{J}$  corresponding to the OLM in Fig. 2 (right). The second column yields the size of the set  $\mathcal{J}$  of matrices  $\hat{J}$  that achieve maximal  $h_E$  in a given interval (4<sup>th</sup> column). The third column lists the connected components in  $\mathcal{J}$  under rewiring of a single negative coupling. The format used is size  $\times$  multiplicity  $+$  ... All models in the same class share the same (ferromagnetic) ground state.

#### 4.1 The mean field Ising ferromagnet and spin glasses

The mean field Ising ferromagnet (MFIFM) corresponds to  $J_{i,j} = J$  for all  $i, j$ . For large  $n$ , this is characterised by a high temperature disordered phase for  $J > J_c/n$  and by a low temperature ordered phase for  $J < J_c/n$  where a non-zero magnetisation spontaneously appears. Notice that the values of the energy for the MFIFM range over an interval  $[-Jn(n-1)/2, -Jn(n-1)/2]$  of order  $n^2$ , but energies  $E_s$  can take at most  $n+1$  different values

$$E_m = -\frac{J}{2}(m^2 - n), \quad m = \sum_{i=1}^n s_i = -n, -n+2, \dots, n-2, n. \quad (19)$$

This implies that  $h_E \leq \log(n+1)/\log n$ . Note also that there is a single matrix  $\hat{J}$  which correspond to the degeneracy of energy levels  $W(E)$  of the MFIFM.

Fig. 3 reports the curves  $h_E(h_s)$  for several values of  $n$ . The curve exhibits a maximum in the neighbourhood of the critical point  $J \approx J_c/n$ . The decreasing part to the right of the maximum corresponds to the high temperature phase, whereas the one to the left of the maximum to the low temperature phase. As  $n$  increases, the maximum shifts to values of  $h_s$  closer and closer to one. At the same time, the maximum gets sharper and sharper and its value slowly decreases towards a finite limit (see inset).

The limiting form of the curve  $h_E(h_s)$  can be computed in the limit  $n \rightarrow \infty$  (see Appendix). This shows that

$$\lim_{n \rightarrow \infty} h_E = \begin{cases} 1/2 & J \neq J_c/n \\ 3/4 & J = J_c/n, \end{cases} \quad (20)$$

which is consistent with the bound  $h_E \leq 1$ . The analysis leading to this result (see Appendix) confirms that  $h_E$  depends on sub-leading contributions that arise from the integration of fluctuations around the saddle point value. At the critical point  $J = J_c/n$ , the resolution converges to  $h_s \rightarrow 1$ . So, the result  $h_E \rightarrow 1/2$  as  $n \rightarrow \infty$  holds in the whole range  $h_s \rightarrow 1/2$ . On the other hand, for  $J = 0$  we have  $h_s = 1$ , exactly. Hence depending on how  $h_s \rightarrow 1$ , all values of  $h_E \in [1/2, 3/4]$  can be achieved. Fig. 3 is fully consistent with this result, although the convergence is very slow. Notice also that the limiting value is approached from above for some values of  $h_s$  and from below for other values.

When  $J_{i,j} = \pm J$  are chosen at random with equal probability, we know that the relevant scale for  $J$  is  $1/\sqrt{n}$ . The ground state energy is extensive so  $E_s$  spans a number of energy levels that is at most of order  $n^{3/2}$ . Therefore we expect that  $h_E \leq 3/2$  for a spin glass. In fact, for  $J = c/\sqrt{n}$  with  $c$  finite but different from the critical point, the distribution of the



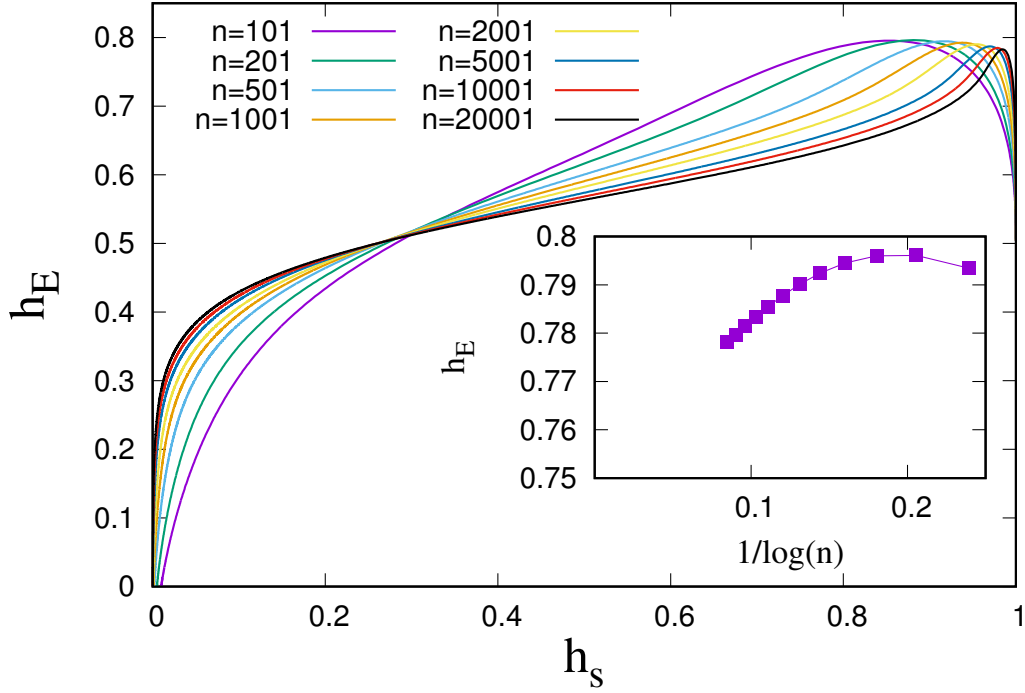


FIGURE 3.  $h_E$  vs  $h_s$  for the MFIFM for  $n = 101, 201, 501, 1001, 2001, 5001, 10001$  and  $20001$ . Inset: maximal value of  $h_E$  as a function of  $1/\log n$ .

energy extends over a range of order  $\delta E \propto \sqrt{n}$ . This suggests that the number of energy levels on which  $p(E)$  is non-zero grows linearly with  $n$ , and hence that  $h_E \rightarrow 1$  as  $n \rightarrow \infty$  for a model with randomly chosen  $J_{i,j}$ . Zero modes at the critical point may yield values  $h_E > 1$ .

## 4.2 The star model

Let us now consider a model that differs from a MFIFM by that fact that one spin has antiferromagnetic interactions with  $\ell < n$  other spins. More precisely,  $J_{i,j} = -1$  if  $i = 1$  and  $j \leq \ell + 1$ , and  $J_{i,j} = +1$  otherwise. We divide the  $n - 1$  group of spins, except spin  $s_1$ , into two groups: the  $\ell$  ones with anti-ferromagnetic interaction with  $s_1$  and the remaining  $n - \ell - 1$ . If  $q$  and  $k$  are the number of positive spins in the first and second group, respectively, the energy is given by

$$\epsilon(k, q, s_1) = J \left[ s_1(n - 1 - 2\ell - 2k + 2q) - \frac{1}{2} (2k + 2q - n + 1)^2 + \frac{n - 1}{2} \right]. \quad (21)$$

The degeneracy of energy levels is given by

$$W(E) = \sum_{k=1}^{n-1-\ell} \sum_{q=1}^{\ell} \sum_{s_1=\pm 1} \binom{\ell}{q} \binom{n-1-\ell}{k} \delta_{E, \epsilon(k, q, s_1)}. \quad (22)$$

Notice that for  $\ell = 0$  one recovers the MFIFM. A gauge transformation  $J_{i,j} \rightarrow \tau_i J_{i,j} \tau_j$ , with  $\tau_1 = -1$  and  $\tau_i = +1$  for  $i > 1$ , maps a model with  $\ell > n/2$  into a model with  $\ell' = n - \ell \leq n/2$ . So it is sufficient to study the model for  $\ell \leq n/2$ .

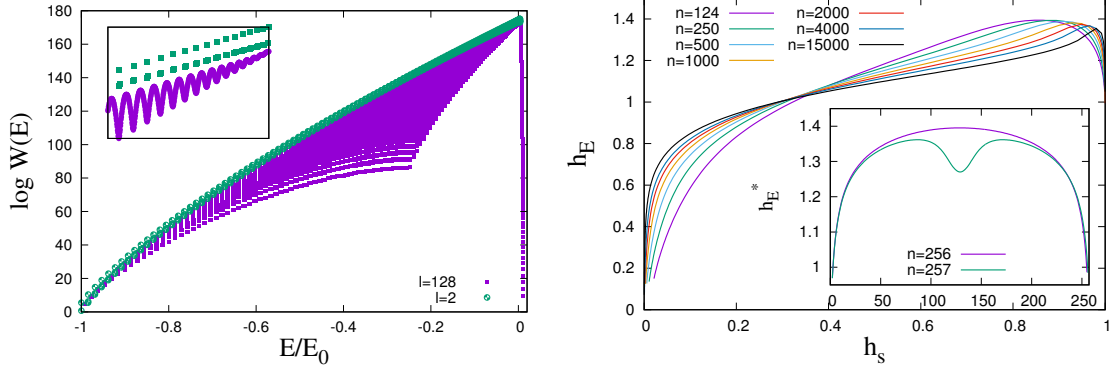


FIGURE 4. (Left) Degeneracy of energy levels for  $n = 256$  and  $\ell = 2$  and  $128$ . Energies are rescaled by  $E_0 = Jn(n-1)/2$ . For  $\ell = 2$  there are 385 distinct energy levels, whereas for  $\ell = 128$  there are 8511. The inset magnifies the data in the range  $E \in [-0.03E_0, 0]$ . (Right) curves  $h_E(h_s)$  for  $\ell = n/2$  (full lines) and different values of  $n$ . Inset: maximal (over  $h_s$ ) value of  $h_E$  as a function of  $\ell$ , for  $n = 256$  and  $257$ .

The degeneracy  $W(E)$  of energy levels is shown in Fig. 4(left) for  $n = 256$ ,  $\ell = 2$  and  $\ell = 128$ . As  $\ell$  increases, the number of different values that  $E$  takes also increases. For  $n = 256$ , the values that  $E$  can take are 129, 385 and 8511 for  $\ell = 0, 2$  and  $128$ , respectively. Indeed, for the MFIFM ( $\ell = 0$ )  $E$  can take only  $n/2 + 1$  different values (for even  $n$ ), whereas for  $\ell = n/2$  we find that the number of possible values of  $E$  grows almost as  $n^2$ . At the same time,  $W(E)$  acquires a rapid variation as a function of  $E$ , so that for large  $n$ ,  $W(E)$  becomes a space filling curve (see Fig. 4 left and inset). Interestingly, the thermodynamics of the model is dominated by the convex envelope of  $\log W(E)$ , which is the same as that of the MFIFM. Therefore the star model and the MFIFM have indistinguishable thermodynamic properties. This is consistent with the fact that the number of  $J_{i,j} = -1$  is a fraction of order  $1/n$  of the total number of interactions and that they impinge on one out of the  $n$  spins. It is easy to check that, for  $\ell \leq n/2$ , the ground state of the star model is the ferromagnetic state  $s_i = s_j$  for all  $i \neq j$ .

The maximal value of  $h_E^*(\ell) = \max_{h_s} h_E$  for even values of  $n$  is achieved at  $\ell = n/2$  (see inset of Fig. 4 right), whereas for odd values of  $n$ ,  $h_E^*$  reaches a lower maximum at  $\ell \approx n/3$ . The symmetry for  $\ell \rightarrow n - \ell$  of these curves is a consequence of the gauge transformation discussed above. The curves  $h_E(h_s)$  for  $\ell = n/2$  and for different values of  $n$  are shown in Fig. 4(right). We find that the highest relevance  $H[E]$  for even  $n$  and  $\ell = n/2$ , grows faster than  $\log n$ . An extrapolation of the maximal value of  $h_E$  is consistent with  $h_E \rightarrow 5/4$  as  $n \rightarrow \infty$ . At fixed values of  $h_s$  instead, we observe a slower growth of  $H[E]$  with  $\log n$ , that may be consistent with  $h_E \rightarrow 1$  for large  $n$ . These values are consistent with the fact that, the degeneracy of each energy level  $E_m$  of the MFIFM is spread over  $n$  other energy levels,  $\sqrt{n}$  of which contribute to  $H[E]$  (see inset of 4 left). This suggests a relation  $h_E^{\text{Star}} = h_E^{\text{MFIFM}} + 1/2$ , that is consistent with our numerical results.

Finally we remark that the set of models with this structure is decomposed into  $n$  subsets, each of which is connected with respect to a single rewiring of a negative  $J_{i,j}$ . Indeed each of the  $\ell$  negative links can be rewired to any of the  $n - \ell - 1$  spins with all ferromagnetic interactions. This dynamics, however, keeps the hub node fixed, so each of the  $n$  possible choices of the hub identifies a connected component. This is consistent with the conjecture that models with high relevance are organised in sets easily accessible by local update dynamics.

### 4.3 A recursive model

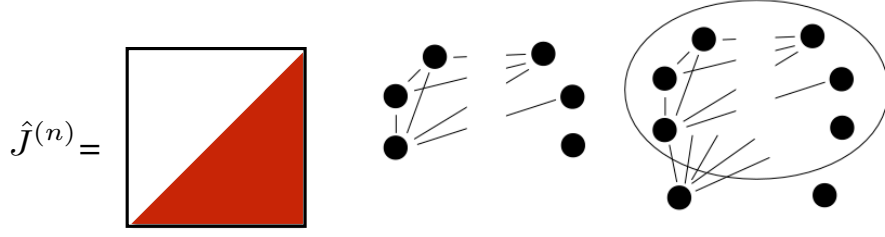


FIGURE 5. Left: Sketch of the structure of the matrix  $\hat{J}$  for structure of recursive models. Red indicates negative  $J_{i,j}$ . Right: sketch of the recursion that relates a model with  $n$  spins to a model with  $n + 2$  spins.

The next architecture that we shall consider is one where  $J_{i,j} = -1$  for  $i > \ell$  and  $j \geq n + \ell - i$ , and  $J_{i,j} = +1$  otherwise. For  $\ell = 1$  this corresponds to a matrix  $\hat{J}$  that has the form shown in Fig. 5(left). In these models, the set of negative  $J_{i,j}$  is organised according to a nested network [14]. These matrices can be obtained through a recursive procedure (see Fig. 5 right): we start from  $n = 2$  with  $J_{1,2} = +1$ . At each iteration, from a system of  $n$  spins, we add two spins,  $s_0$  and  $s_{n+1}$ . The spin  $s_0$  has  $J_{0,j} = -1$  with all other spins  $j \leq n$ . The spin  $s_{n+1}$  has  $J_{i,n+1} = -1$  with all spins, including  $s_0$ . This generates a matrix with  $n + 2$  spins with the desired structure.

For each state at energy  $E$  and magnetisation  $M = \sum_{i=1}^n s_i$ , and each choice of  $s_0, s_{n+1}$ , we obtain a state of the system with  $n + 2$  spins with energy

$$E' = E - J [s_0 s_{n+1} - s_0 M + s_{n+1} M] \quad (23)$$

and magnetisation  $M' = M + s_0 + s_{n+1}$ . Thus the energy degeneracy of a system of  $n$  spins can be computed as

$$W_n(E) = \sum_M w_n(E, M) \quad (24)$$

where  $w_n$  satisfies the recursive equation

$$w_{n+2}(E', M') = \sum_{s_0, s_{n+1} = \pm 1} \sum_{E, M} w_n(E, M) \delta_{E'(E)} \delta_{M', M+s_0+s_{n+1}} \quad (25)$$

where the shorthand  $\delta_{E'(E)}$  reduces the sum to only those terms where Eq. (23) is satisfied.

It is possible to generalise the recursion relation to obtain matrices with different values of  $\ell$ . For example, the case  $\ell = n/2$  can be obtained by separating the set of spins into two equal parts,  $\mathcal{I}_{\leq} = \{i \leq n/2\}$  and  $\mathcal{I}_{>} = \{i > n/2\}$ . To each of the two sets we add two spins at each iteration, thereby obtaining a system with  $n + 4$  spins. Of the two spins added to  $\mathcal{I}_{\leq}$ , one has  $J_{0,j} = -1$  with all spins  $j \in \mathcal{I}_{\leq}$  and  $J_{0,j} = +1$  for all  $j \in \mathcal{I}_{>}$ . The other three spins have ferromagnetic interactions with all other spins, as well as among themselves. It is easy to see by induction, that the ground state of this model is the ferromagnetic one  $s_i = s_j$  for all  $i, j$ . This holds true for all  $\ell \leq n/2$ .

Numerical iteration of the recursion relations allowed us to compute the degeneracy  $W_n(E)$  and the curves  $h_E(h_s)$  for different values of  $n$  and  $\ell$ . We observed that, for a given system size  $n$ , the maximal relevance for these models is obtained for  $\ell = n/2$ . Fig. 6 shows the results for different values of  $n$  and for  $\ell = 1$  (left) and  $n/2$  (right).

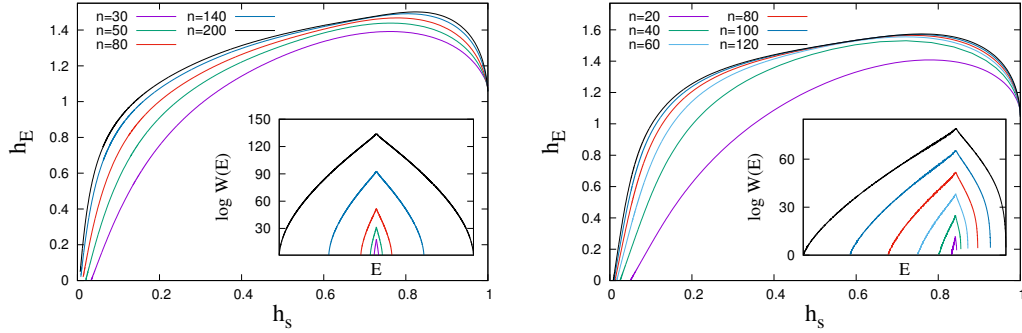


FIGURE 6. Relevance  $h_E$  as a function of  $h_s$  for the recursive model with  $\ell = 1$  (left) and  $\ell = n/2$  (right), for different values of  $n$  (see legend). The inset shows the degeneracy  $\log W(E)$  as a function of  $E$  for the corresponding models.

Although we could not access values of  $n$  as large as in the previous cases, Fig. 6 shows that this model has qualitatively distinct features. First, we found that  $\log W(E)$  approaches a continuous function of  $E$  and it has support on a number of energy levels that increases as  $n^2$ . For  $\ell = 1$  we found that  $W(E) = W(-E)$  is a symmetric function of  $E$  (see inset, left). Second, in both cases, we found that  $h_E$  increases monotonically with  $n$  and it approaches a limiting value already for relatively small values of  $n$ . The maximal limiting values of  $h_E$  is higher than that achieved with the other architectures. We note that the number of anti-ferromagnetic interactions in these models is proportional to  $n^2$ , and hence their thermodynamic properties in the  $n \rightarrow \infty$  limit differ from those of the MFIFM.

For a given value of  $\ell$ , there are  $\frac{n!}{(n-\ell)!}$  possible models depending on how the set of  $n - \ell$  fully ferromagnetic spins are chosen and on the ranking of the  $\ell$  spins. This set of models forms a single connected component under a single rewiring of a  $J_{i,j} = -1$ <sup>6</sup>, which is again consistent with the conjecture that OLM are easily accessible by local updates of the couplings.

## 5 Conclusion

The OLM discussed in this paper corresponds to an ideal limit that internal representations of well trained learning machines is expected to approach. This is because the relevance  $H[E]$  provides a lower bound to the mutual information between the state of the machine and the hidden features that a learning machine is supposed to extract (see Section 1). The principle of maximal relevance then pushes the architecture of the learning machine to detect maximally informative features. This result is a characterisation of typical learning machines. It does not excludes the existence of efficient learning machines with low values of  $H[E]$ . Rather it insures that learning machine with highest value of  $H[E]$  provide at least that much information on the hidden features.

A distinctive feature of this approach is that it allows us to discuss the properties of OLMs without any reference to the data they have been trained with, as long as this is suf-

<sup>6</sup>In order to show this, let  $\partial_i$  be the set of spins with  $J_{i,j} = -1$ . If we sort spins in such a way that  $\delta_1 = (1, \dots, \ell)$ ,  $\delta_2 = (1, \dots, \ell-1), \dots, \delta_k = (1, \dots, \ell-k+1), \dots$ , then the rewiring of the link  $(k, \ell-k+1)$  to  $(k+1, \ell-k+1)$  interchanges the order of spins  $k$  and  $k+1$  in the hierarchy. The rewiring of the link  $(1, \ell)$  to  $(1, k)$  with  $k > \ell$  changes the membership of spins in the network connected by  $J_{i,j} = -1$ . Repeated application of these two moves in the appropriate order makes it possible to reach any model in the set from any other model.

ficiently structured. The peculiar statistical mechanics properties of systems that achieve maximal relevance has already been discussed in Ref. [15]. The contribution of this paper is to investigate this limit in the context of a well defined class of models – the fully connected Ising models with binary couplings. Compared to architectures actually used in deep learning, this is manifestly a toy model. Yet it sheds light on the properties responsible for the spectacular performance of learning machines, contributing to the literature on the statistical mechanics of learning [3, 4, 6, 7]. First, we argue that these properties are related to sub-extensive quantities in the statistical mechanics treatment. This on one side suggests that learning machines are characterised by properties that may not be accessible to a statistical mechanics treatment. A proper understanding of these systems requires a detailed analysis of fluctuations around the saddle point. On the other, this result tallies with observation that complexity reveals itself in the sub-extensive contribution to the entropy, both in statistical models<sup>7</sup> [16, 17] and in time series<sup>8</sup> [18]. Second, we find that in Ising OLMs the majority of the interactions are positive and the negative ones are distributed unevenly across the sites. This implies that their ground state is ferromagnetic (in the fixed gauge adopted here), and the wide distribution of energy levels implies that it sits on a wide minimum (in the space  $s$  of configurations), as observed in [9]. Each OLM are realised by a set of interaction matrices  $\mathcal{J}$  with a large degeneracy. Local update rule that imply the rewiring of a single negative coupling can explore a large part of this set, showing that the relevance  $H[E]$  is characterised by wide flat maxima in the space of the parameters  $\hat{J}$ . It is tempting to relate this property to that discussed in Ref. [4].

Finally, our results contributes to the discussion on the criticality of learned models [6, 19]. We confirm that models such as the MFIFM or the star model, have a superior learning performance when poised at the critical point [20]. Yet, it is not strictly necessary for an OLM to be poised at a critical point marking the transition between two different phases. Yet, we exhibited models with a learning performance higher than that of models that feature a phase transition, in a wide range of the resolution scale. This corroborates the thesis [9] that statistical criticality is an intrinsic and generic characteristic of OLM.

We hope that these results will not only contribute to our understanding of learning machines, but that they may also pave the way to applications that may improve further the performance of learning machines.

## A Asymptotic value of $h_E$ for the MFIFM

The distribution of energy levels is given by  $p(E) = W(E)e^{-E}/Z$ , where  $Z = \sum_E W(E)e^{-E}$ . Hence the relevance is given by

$$H[E] = \log Z - \langle \log W(E) \rangle + \langle E \rangle. \quad (26)$$

The degeneracy of energy level  $E_m$  in Eq. (19) is

$$W(E_m) = 2 \binom{n}{\frac{n+m}{2}} \simeq \sqrt{\frac{2}{\pi n(1-\mu^2)}} e^{nS(\mu)}, \quad \mu = \frac{m}{n} \in [-1, 1]$$

<sup>7</sup>Minimum Description Length, as well as Bayesian inference, identify the leading order term that should be used in model selection to penalise the likelihood of models for their complexity. In both cases this term is  $\frac{d}{2} \log N$ , where  $d$  is the number of parameters of the model and  $N$  is the number of data points. This term is sub-leading with respect to the log-likelihood, which is proportional to  $N$ .

<sup>8</sup>The complexity of a time series is defined in [18] as the predictive information, which is the mutual information between the recent past, in a window of  $T$  time points, and the future of the time series.

where  $S(\mu) = -\frac{1+\mu}{2} \log \frac{1+\mu}{2} - \frac{1-\mu}{2} \log \frac{1-\mu}{2}$ . In the regime where  $h_s \in [0, 1]$  is finite,  $J$  is of order  $1/n$  and, for  $n \rightarrow \infty$ , the partition function is dominated by the saddle point  $\mu^* = \arg \min_{\mu} f(\mu)$  with  $f(\mu) = Jn\mu^2/2 - S(\mu)$ . For  $Jn \neq 1$ , the first term in Eq. (26) can be computed with integration over the gaussian fluctuations

$$Z \simeq \sqrt{\frac{2n}{\pi}} \int_{-1}^1 \frac{d\mu}{\sqrt{1-\mu^2}} e^{-nf(\mu)} \simeq \sqrt{\frac{2}{\pi(1-\mu^{*2})f''(\mu^*)}} e^{-nf(\mu^*)}$$

Here, the  $\sqrt{n}$  factor is canceled because  $f(\mu) - f(\mu^*) \sim (\mu - \mu^*)^2$ , and the change of variables  $z = \sqrt{n}(\mu - \mu^*)$  generates a  $1/\sqrt{n}$  term.

Hence  $\log Z \simeq -nf(\mu^*) + \text{const.}$  The extensive term in  $\log Z$  is canceled by an analogous term in

$$\langle \log W(E) \rangle - \langle E \rangle \simeq nf(\mu^*) + \log \sqrt{2\pi n(1-\mu^2)}$$

so, to leading order,  $H[E] \simeq \frac{1}{2} \log n + \text{const.}$  which implies  $h_E \rightarrow 1/2$  as  $n \rightarrow \infty$ .

For  $Jn = 1$ , instead,  $f(\mu) - f(\mu^*) \simeq a(\mu - \mu^*)^4 + \dots$ . This implies that in the calculation of  $Z$  we need a change of variables  $z = n^{1/4}(\mu - \mu^*)$  that yields  $\log Z \simeq \frac{1}{4} \log n + \text{const.}$  This additional term is responsible for the asymptotic behaviour  $h_E \rightarrow 3/4$  for  $Jn = 1$ .

## References

- [1] John J. Hopfield. Neural networks and physical systems with emergent collective computational abilities. *Proc Natl Acad Sci U S A*, 79(8):2554–8, 1982.
- [2] David H. Ackley, Geoffrey E. Hinton, and Terrence J. Sejnowski. A learning algorithm for boltzmann machines\*. *Cognitive Science*, 9(1):147–169, 1985.
- [3] Jrme Tubiana, Simona Cocco, and Rmi Monasson. Learning compositional representations of interacting systems with restricted boltzmann machines: Comparative study of lattice proteins. *Neural Computation*, 31(8):1671–1717, 2019.
- [4] C. Baldassi, C. Borgs, J. T. Chayes, A. Ingrosso, C. Lucibello, L. Saglietti, and R. Zecchina. Unreasonable effectiveness of learning neural networks: From accessible states and robust ensembles to basic algorithmic schemes. *Proceedings of the National Academy of Sciences*, 113(48):E7655–E7662, 2016.
- [5] Marc Mézard. Mean-field message-passing equations in the hopfield model and its generalizations. *Phys. Rev. E*, 95:022117, Feb 2017.
- [6] M. E. Rule, M. Sorbaro, and M. H. Hennig. Optimal encoding in stochastic latent-variable Models. *ArXiv e-prints*, page arXiv:1802.10361, February 2018.
- [7] A. Decelle, G. Fissore, and C. Furtlehner. Thermodynamics of restricted boltzmann machines and related learning dynamics. *Journal of Statistical Physics*, 172(6):1576–1608, Sep 2018.
- [8] Marco Baity-Jesi, Levent Sagun, Mario Geiger, Stefano Spigler, Gerard Ben Arous, Chiara Cammarota, Yann LeCun, Matthieu Wyart, and Giulio Biroli. Comparing dynamics: Deep neural networks versus glassy systems. In Jennifer Dy and Andreas Krause, editors, *Proceedings of the 35th International Conference on Machine Learning*, volume 80 of *Proceedings of Machine Learning Research*, pages 314–323, StockholmLssan, Stockholm Sweden, 10–15 Jul 2018. PMLR.



- [9] Ryan John Cubero, Junghyo Jo, Matteo Marsili, Yasser Roudi, and Juyong Song. Statistical criticality arises in most informative representations. *Journal of Statistical Mechanics: Theory and Experiment*, 2019(6):063402, jun 2019.
- [10] J Song, M Marsili, and J Jo. Resolution and relevance trade-offs in deep learning. *Journal of Statistical Mechanics: Theory and Experiment*, 2018(12):123406, dec 2018.
- [11] Ryan Cubero, Matteo Marsili, and Yasser Roudi. Minimum description length codes are critical. *Entropy*, 20(10):755, Oct 2018.
- [12] D J Schwab, I Nemenman, and P Mehta. Zipf’s law and criticality in multivariate data without fine-tuning. *Phys. Rev. Lett.*, 113:068102, Aug 2014.
- [13] T M Cover and J A Thomas. *Elements of information theory*. John Wiley & Sons, 2012.
- [14] Samuel Jonhson, Virginia Domnguez-Garca, and Miguel A. Muñoz. Factors determining nestedness in complex networks. *PLoS One*, 8(9):e74025, 2013.
- [15] M. Marsili. The peculiar statistical mechanics of Optimal Learning Machines. *ArXiv e-prints*, page arXiv:1904.09144, February 2018.
- [16] G Schwarz. Estimating the dimension of a model. *Ann. Statist.*, 6(2):461–464, 03 1978.
- [17] In Jae Myung, Vijay Balasubramanian, and Mark A. Pitt. Counting probability distributions: Differential geometry and model selection. *Proceedings of the National Academy of Sciences*, 97(21):11170–11175, 2000.
- [18] W Bialek, I Nemenman, and N Tishby. Predictability, complexity, and learning. *Neural Computation*, 13(11):2409–2463, 2001.
- [19] M A Muñoz. Colloquium: Criticality and dynamical scaling in living systems. *Rev. Mod. Phys.*, 90:031001, Jul 2018.
- [20] I Mastromatteo and M Marsili. On the criticality of inferred models. *Journal of Statistical Mechanics: Theory and Experiment*, 2011(10):P10012, 2011.